



Design, Synthesis and Evaluation of Functionalized Azaglycinamides as Cytotoxic and Antinociceptive Agents

Arifa Begum Shaik^{*a}, Shaheen Begum^b, Sujatha Dodoala^b, Bharathi Koganti^b

^aBharat Institute of Technology, Ibrahimpatnam, Rangareddy, Affiliated to Jawaharlal Nehru Technological University Hyderabad, Telangana, India, ^bInstitute of Pharmaceutical Technology, Sri Padmavati Mahila Visvavidyalayam, Tirupati, Andhra Pradesh, India.

Abstract

Aza analogs of peptides are used in the treatment of cancer and neurodegenerative disorders. The clinical approval of goserelin for the treatment of prostate cancer proves the therapeutic potentiality of azaglycine residue. With this background, a novel approach to functionalizing the azaglycine moiety aimed at compounds possessing C-functionalization with active five membered heterocycles (pyrrole, imidazole, etc thiazolidine-2, 4-dione) and N-functionalization with acyl chains on azaglycine moiety were synthesized. The compounds were evaluated for *in vitro* MAGL inhibition and cytotoxicity against MCF-7 cell lines. The biological activities were corroborated with molecular docking studies with Cathepsin B and MAGL enzymes. The compounds with prominent *in vitro* and *in silico* potential against MAGL were evaluated for antinociceptive activity. This privileged N- and C-functionalization approach in the synthesis of azaglycinyl analogs demonstrated that N-oleoyl and C-thiazolidine-2,4-dione functionalized azaglycinamide derivative **1q**, was found to possess moderate cytotoxic and MAGL inhibitory profile. The active compounds were well accommodated in the binding sites of these targets with good electrostatic complementarity. The N-oleoyl and C-thiazolidine-2, 4-dione functionalized azaglycine can be envisaged as a novel molecule with potential anticancer and antinociceptive activities.

Keywords: Azaglycinamides, N- and C- functionalization, MAGL Inhibition, Antinociception, Cytotoxicity.

Corresponding Authors: Arifa Begum Shaik, Bharat Institute of Technology, Ibrahimpatnam, Rangareddy, Affiliated to Jawaharlal Nehru Technological University Hyderabad, Telangana, India
Tel: 8555045478
Email: arifa.medchem@gmail.com

Cite this article as Shaik A. B., Begum S, Dodoala S, Koganti B, Design, Synthesis and Evaluation of Functionalized Azaglycinamides as Cytotoxic and Antinociceptive Agents, 2021, 17 (2): 129-158.

1. Introduction

Peptidomimetics, the attractive tools in drug design, provide improved bioavailability, metabolic stability, and receptor selectivity compared to native natural peptides [1]. Among the various structural variants of peptidomimetics designed and synthesized, the backbone modifications serve as interesting

peptidomimetic modification due to their diversified biological and pharmacokinetic properties (Figure 1). Azapeptides, azadepsipeptides, β - and γ -peptides, aminoxypeptides, and hydrazinopeptides are the well-established backbone modifications [2]. Azaamino acids serve as an attractive tool for drug design leading to the development of azapeptides as the most useful peptidomimetic drug candidates.

Glycine containing peptides were reported to be metabolically stable as glycine is involved in close and specific interaction with the receptor by the absence of a sterically hindered side chain. The replacement of tetrahedral carbon, C $^{\alpha}$ of glycine with trivalent N, generates the privileged azaamino acid, azaglycine. Replacement of glycine with azaglycine increases the number of interfacial cross-strand hydrogen bonds (Figure 2). The azaglycine was suggested to impose a bent like structure that positioned the lipophilic moieties in a bioactive conformation critical for high activity and selectivity towards the target receptor or enzyme [3].

The clinical approval of the azaglycine peptide analog, goserelin for prostate cancer treatment proves the therapeutic potentiality of azaglycine residue. Another azaglycine analog, atazanavir, received FDA approval to treat prostate cancer, breast cancer, and HIV infections [4, 5].

Incorporating an azaamino acid makes azapeptides more rigid than their peptide analogs due to the inability of the N-CO- bond to rotate at the P₁ site (Figure 3). This feature

makes azapeptides ideal enzyme inhibitors viz: protease inhibitors (cysteine proteases, serine proteases, and aspartic proteases). Uncontrolled proteolysis is observed in cancers such as multiple melanomas (MM) and non-Hodgkin's lymphoma (NHL). The inhibition of protease leads to the death of cancerous cells. Hence azaamino acid derivatives can be utilized for various protease targeted therapies viz: cardiovascular, inflammatory, and infectious diseases like HIV, cancer, and neurodegradative disorders [6, 7].

Modulation of endocannabinoids, arachidonoyl ethanolamide (AEA), and 2-arachidonoyl glycerol (2-AG) constitutes a therapeutic approach for cancer, inflammation, and nociception. Development of inhibitors monoacylglycerol lipase (MAGL) is considered as the most promising therapeutic approach, for the treatment of various neurological diseases, inflammation, pain and other pathological states [8]. MAGL inhibition leads to a reduction of free fatty acids (FFAs) and lysophosphatidic acid (LPA), and thereby attenuate cancer cell pathogenicity (Figure 4). Transient receptor potential ankyrin 1 (TRPA1) plays a crucial role in pain management, mediating AEA's effects [9]. These findings suggest that targeting MAGL and TRPA1 channel attracts the current drug development of novel antinociceptive and anticancer agents.

Incorporation of heterocyclic scaffolds is known to impart conformational restriction into the designed peptides and peptidomimetics, which has focused on drug design. Peptidomimetics comprising heterocyclic

moieties display a considerable therapeutic role as antitumor, antibacterial, antiviral, anti-inflammatory, antimicrobial agents. The aromatic heterocycles such as pyrrole, tetrazole, triazole, and pyrazoles are used as cis-peptide bond mimics.

The pyrrole derivatives possess a hydrogen bond donor that may mimic the amide NH to favor β -strand geometry [10]. Imidazole nucleus, one of the promising heterocyclic mimics, presents a plethora of substitution patterns favoring the design of different derivatives possessing diverse biological significance. Dacarbazine, an imidazole carboxamide, is used for the treatment of metastatic melanoma [11].

Thiazolidine-2,4-dione (TZD) analogs have been recognized as the privileged templates in drug discovery, and synthesis of thiazolidine derivatives remains promising in medicinal chemistry, despite their non-selectivity in binding to multiple targets [12]. Drugs containing the core five-membered heterocyclic rings like pyrrole, imidazole, and thiazolidinediones include Lipitor, ondansetron, azathioprine, cozaar, and glitazones.

Inspired by the significance of the azaglycinyl amino acid and heterocyclic conformational constraints such as pyrrole, imidazole, and thiazolidine 2, 4-dione ring systems in the design of peptidomimetics, it was aimed to synthesize and evaluate various azaglycinamide derivatives with both N-terminal and C-terminal functionalization on

the azaglycinyl moiety ([Figure 5](#)) for cytotoxicity and antinociceptive activity.

2. Materials and Methods

2.1. Chemistry

2.1.1. General

Ethylchloroformate, pyrrole, imidazole, oleic acid, palmitic acid, hydrazine hydrate, acetylhydrazide, benzhydrazide, and Ally Isothiocyanate (AITC) were procured from Merck Ltd, Mumbai, India. All other reagents and solvents were of AR grade and were purchased from SD Fine Chemicals Limited, India. Carousel 6 plus station from Radleys UK was used for parallel synthesis. Melting points were determined in an open capillary tube in the Sigma melting point apparatus and are uncorrected. Infrared Spectra of the compounds were obtained on a Bruker FTIR spectrophotometer, ^1H NMR Spectra was recorded on Bruker Avance, 400 MHz. Mass spectrums were obtained from Apex Mass spectrum (300800.D).

DMEM (Dulbecco's modified Eagles medium), MTT [3-(4, 5-dimethylthiazol-2-yl)-2, 5-diphenyl tetrazolium bromide], trypsin, EDTA Phosphate Buffered Saline (PBS) and were purchased from Sigma Chemicals Co. (St. Louis, MO) and Fetal Bovine Serum (FBS) was purchased from Gibco. T-25, T-75 culture flasks, and 96 well plates were purchased from Eppendorf India. MAGL inhibitor screening assay kit was purchased from Cayman chemicals (Kit no. 700037, Ann Arbor, MI-USA).

2.1.2. Procedure for the Synthesis of Substituted Hydrazides A-F

Synthesis of cinnamic acid hydrazide C:

To a solution of cinnamic acid (1.49 g, 0.01mol) in methanol (20 mL), concentrated sulphuric acid (0.5mL) was added, and the reaction mixture was refluxed for 12 hrs. The reaction mixture was distilled and the product was and treated with a saturated sodium bicarbonate solution to give the desired methyl ester.

To the solution of appropriate methyl ester of cinnamic acid (1.62 g, 0.01mol) in methanol (150 mL) 95% hydrazine hydrate (0.5 mL, 0.01mol) was added and the mixture was refluxed for 8-9 hrs. The reaction mixture was poured on to the ice, and the product was recrystallized from ethanol [13]. FTIR (KBr) cm^{-1} : 3489.18(N-H, str), 3371.38 and 3305 (N-H, anti sym str and sym str), 2900-2897 (Ar-CH, str), 1649.99 (C=O, str), 1489.06 (-CH₂, str), 802.79 (N-H, bend). A similar procedure was followed for synthesis of other hydrazides A, B, D, E, & F by treating corresponding acid methyl ester with hydrazine hydrate.

2.1.3. General Method of Synthesis of Ethyl 1H-pyrrole-1-carboxylate, Ethyl 1H-imidazole-1-carboxylate and Ethyl Carboxylate of Thiazolidine-2, 4-dione

To a solution of pyrrole (0.7ml, 0.01mol) or imidazole (0.7 g, 0.01mol) or thiazolidine-2, 4-dione (0.6 g, 0.01mol) in dichloromethane (50 mL), triethylamine (1mL) was added. The stirring was continued for 3-5 hrs with

simultaneous addition of ethyl chloroformate (1.26 mL, 0.01mol) [14].

2.1.4. General Method of Synthesis of N'-Substituted-1H-pyrrole-1-carbohydrazides (1a to 1f), N'-(1-iminoethyl)-1H-imidazole-1-Carbohydrazides (1g to 1l) and N'-substituted-2, 4-dioxothiazolidine-3-carbohydrazides (1m to 1r)

To a solution of appropriate ethyl carboxylate (0.01mol) in 50 ml of ethanolic solution, substituted hydrazide (0.02mol) was added, and the mixture was refluxed for 4-6 hrs. The products were recrystallized from methanol.

N'-(1-iminoethyl)-1H-pyrrole-1-carbohydrazide, (1a): FTIR (KBr) cm^{-1} 3281.73(N-H str), 2926.78(C-H aromatic str), 2844.64(C-H aliphatic str), 1786.26(C=O str), 1672.86(C=O str of amide), 1598.22(C=C), 1489.78(C-N str), 856.32(C-H aromatic bend); ¹H NMR(400 MHz, DMSO-d₆, δ) 8.03-8.22 (d, J=7.6Hz, 2H, NH-NH of hydrazide), 6.23-7.52 (m, 4H, pyrrole), 2.07 (s, 3H, COCH₃), MS(EI) m/z 167.40[M]⁺, 168.40 [M+H]⁺ Anal. C 50.20; H, 5.42; N, 25.13

N'-benzoyl-1H-pyrrole-1-carbohydrazide, (1b): FTIR (KBr) cm^{-1} 3199.90(N-H str), 3002.40(C-H aromatic str), 2859.29 (C-H aliphatic str), 1724.99 (C=O str), 1615.80(C-H aromatic bend), 1541.30(C=C), 1489.10(C-N str), 876.90 (C-H aromatic bend); ¹H NMR(400 MHz, DMSO-d₆, δ) 8.08-8.27 (d, J=7.6Hz, 2H, NH-NH of hydrazide), 7.56-7.62 (m, 3H, Ar-H), 6.23-7.52 (m, 4H, pyrrole);

MS(EI) m/z 229.60[M]⁺, 230.40 [M+H]⁺ Anal. C 62.75; H, 4.85; N, 18.30

N'-cinnamoyl-1*H*-pyrrole-1-carbohydrazide, (1*c*): FTIR (KBr) cm^{-1} 3186.93(N-H str), 3010.34 (C-H aromatic str), 2847.23 (C-H aliphatic str), 1736.87 (C = O str), 1622.76(C=O str of amide), 1549.34(CH=CH), 1482.05 (C-N str) 842.51 (C-H aromatic bend); ¹H NMR(400 MHz, DMSO-d₆, δ) 8.03 (d, J=7.8Hz, 2H, NH-NH of hydrazide), 7.33-7.60 (m, 6H, Ar-H&C=CH _{β}), 7.28-7.30 (m, 2H, pyrrole), 6.89 (d, 1H, J=15.6Hz, CH _{α} =C), 6.27-6.30 (m, 2H, pyrrole), MS(EI) m/z 255.40[M]⁺, 256.50[M+H]⁺ Anal. C 65.72; H, 5.12; N, 16.44

N'-(2-phenoxyacetyl)-1*H*-pyrrole-1-carbohydrazide, (1*d*): FTIR (KBr) cm^{-1} 3326.02(N-H str), 2927.00 (C-H aromatic str), 2850.90 (C-H aliphatic str), 1691.97 (C = O str), 1598.18(C=C), 1412.35 (C-N str), 1230.65 (C-O phenoxy str). 887.19 (C-H aromatic bend); ¹H NMR (400 MHz, DMSO-d₆, δ) 8.00 (d, J=7.6Hz, 2H, NH-NH of hydrazide), 6.27-7.34 (m, 9H, Ar-H& pyrrole); 4.63 (s, 2H, O-CH₂), MS (EI) m/z 259.60[M]⁺, 260.40[M+H]⁺ Anal. C, 60.11; H, 5.04; N, 16.19

N'-oleoyl-1*H*-pyrrole-1-carbohydrazide, (1*e*): FTIR (KBr) cm^{-1} 3400.34(N-H str), 2922.25 (C-H aromatic str), 2852.81 (C-H aliphatic str), 1734.06 (C = O str), 1629.90(C=O str of amide), 1581.68(C=C), 1456.30 (C-N str) 1436.24(CH₂-bend), 1344.43 (CH₃-bend); 889.21 (C-H aromatic bend); ¹H NMR(400 MHz, DMSO-d₆, δ) 8.45-8.64 (d, J=7.6Hz, 2H, NH-NH of hydrazide),

7.67-7.80(m, 4H, pyrrole), 3.40 (m,6H, olefinic & allylic), 1.00-1.19 (m, 23H, CH₂), 0.88-0.91 (t, 3H, CH₃), MS(EI) m/z 388.00 [M-H]⁺ Anal. C 70.85; H, 10.08; N, 10.75

N'-palmitoyl-1*H*-pyrrole-1-carbohydrazide, (1*f*): FTIR (KBr) cm^{-1} 3421.62(N-H str), 2928.19 (C-H aromatic str), 2846.80 (C-H aliphatic str), 1745.10 (C = O str), 1633.87(C=O str of amide), 1592.73(C=C), 1447.34(C-N str) 1429.19(CH₂-bend), 1349.38 (CH₃-bend); 876.16 (C-H aromatic bend); ¹H NMR (400 MHz, DMSO-d₆, δ) 8.25-8.44 (d, J=7.6Hz, 2H, NH-NH of hydrazide); 7.52-7.66 (m, 4H, pyrrole), 2.38 (t, 2H, CH₂), 1.27-1.58 (m, 26H, CH₂), 0.87-0.91 (t, 3H, CH₃), MS(EI) m/z 363.10[M]⁺, 365.90[M+2H]⁺ Anal. C 69.27; H, 10.23; N, 11.54

N'-(1-iminoethyl)-1*H*-imidazole-1-carbohydrazide, (1*g*): FTIR (KBr) cm^{-1} 3339.13(N-H str), 2944.20 (C-H aromatic str), 2839.68 (C-H aliphatic str), 1673.12 (C = O str), 1642.78(C=O str of amide), 1574.20(C=C), 1442.37 (C-N str), 882.35 (C-H aromatic bend); ¹H NMR (400 MHz, DMSO-d₆, δ) 8.39 (m, 1H, CH=N, imidazole); 8.12-8.30(d, J=7.2Hz 2H, NH-NH of hydrazide), 7.46 (dd, 1H, imidazole), 7.15 (dd, 1H, imidazole), 2.08 (s, 3H, CH₃), MS(EI) m/z 168.60 [M]⁺, 169.30[M+H]⁺ Anal. C 42.90; H, 4.81; N, 33.30

N'-benzoyl-1*H*-imidazole-1-carbohydrazide, (1*h*): FTIR (KBr) cm^{-1} 3208.18(N-H str), 3021.62 (C-H aromatic str), 2482.40 (C-H aliphatic str), 1719.62 (C = O str), 1650.07(C=O str of amide), 1534.61(C=C), 1486.22 (C-N str), 888.05 (C-

H aromatic bend); $^1\text{H NMR}$ (400 MHz, DMSO- d_6 , δ) 9.77-9.79(m, 1H, CH=N, imidazole); 9.18(d, $J=7.6\text{Hz}$ 2H, NH-NH of hydrazide), 7.43-7.96(m, 7H, Ar-H & NH-NH of hydrazide), MS(EI) m/z 231.00[M+H] $^+$, 232.00[M+2H] $^+$ Anal. C 57.43; H, 4.37; N, 24.33

N'-cinnamoyl-1H-imidazole-1-carbohydrazide, (1i): FTIR (KBr) cm^{-1} 3224.47(N-H str), 2945.36 (C-H aromatic str), 2886.46 (C-H aliphatic str), 1714.02 (C = O str), 1538.21(C=C), 1442.34 (C-N str), 864.40, (C-H aromatic bend); $^1\text{H NMR}$ (400 MHz, DMSO- d_6 , δ) 8.78-8.80(m,1H,CH=N, imidazole); 7.51(m, 2H, imidazole), 7.66(d, $J=7.6\text{Hz}$ 2H,NH-NH of hydrazide), 7.31-7.34(s, 6H, Ar-H&C=CH $_{\beta}$), 6.42(d, $J=15.6\text{Hz}$, 1H, CH α =C), MS(EI) m/z 256.00[M] $^+$, 258.00[M+2H] $^+$ Anal C 60.84; H, 4.71; N, 21.89.

N'-(2-phenoxyacetyl)-1H-imidazole-1-carbohydrazide, (1j): FTIR (KBr) cm^{-1} 3190.90(N-H str), 3031.60 (C-H aromatic str), 2937.39 (C-H aliphatic str), 1734.28 (C = O str), 1595.83 (C=C), 1493.12 (C-N str), 1235.62 (C-O phenoxy str). 833.90 (C-H aromatic bend); $^1\text{H NMR}$ (400 MHz, DMSO- d_6 , δ) 9.10-9.12(m, 1H, CH=N, imidazole), 6.96-7.33(m,9H,ArH&imidazole&NH-NH of hydrazide 4.01(s,2H,OCH $_2$),MS(EI) m/z 260.00[M] $^+$ Anal. C 55.29; H, 4.62; N, 21.51

N'-oleoyl-1H-imidazole-1-carbohydrazide, (1k): FTIR (KBr) cm^{-1} 3351.01(N-H str), 2944.28 (C-H aromatic str), 2839.62 (C-H aliphatic str), 1673.09 (C = O str), 1648.13(C=C), 1442.46 (C-N str),

1410.14(CH $_2$ -bend), 1362.19 (CH $_3$ -bend), 879.31 (C-H aromatic bend); $^1\text{H NMR}$ (400 MHz, DMSO- d_6 , δ) 8.40-8.42(m, 1H, CH=N, imidazole), 7.39-7.41(m,4H, imidazole & NH-NH of hydrazide), 5.42(d,2H,CH=CH), 2.12-2.15(m,4H,CH $_2$), 1.02-1.50(m,24H,CH $_2$),0.88(s,3H,CH $_3$), MS(EI) m/z 391.20[M+H] $^+$ Anal. C 67.59; H, 9.80 N, 14.33

N'-palmitoyl-1H-imidazole-1-carbohydrazide, (1l): FTIR (KBr) cm^{-1} 3325.18(N-H str), 2925.51 (C-H aromatic str), 2893.63 (C-H aliphatic str), 1673.12(C=O str), 1641.21(C=C), 1435.27(C-N str), 1408.27(CH $_2$ -bend), 1352.22 (CH $_3$ -bend) 877.36 (C-H aromatic bend); $^1\text{H NMR}$ (400 MHz, DMSO- d_6 , δ) 8.40-8.42(m, 1H, CH=N, imidazole); 7.30-7.41(m,4H, imidazole & NH-NH of hydrazide), 2.39(t,2H,CH $_2$), 1.02-1.50(m,26H,CH $_2$), 0.88(t, 3H, CH $_3$),MS(EI) m/z 364.80 , [M] $^+$, 366.60[M+2H] $^+$ Anal. C 65.81; H, 9.90; N, 15.36

N'-acetyl-2,4-dioxothiazolidine-3-carbohydrazide, (1m): FTIR (KBr) cm^{-1} 3121.45 (N-H str), 2934.71 (C-H aromatic str), 2205.13 (C-H aliphatic str), 1712.25 (CO-NHCO), 1654.76 (C=O str), 1536.24 (C=O str of amide), 1475.53(C-N aliphatic str), 876.43(C-H aromatic bend), 679.05 (C-S str); $^1\text{H NMR}$ (400 MHz, DMSO- d_6 , δ) 8.41 (s, 1H, NH of hydrazide); 6.27 (s, 1H, NH of hydrazide), 4.16 (s, 2H, S-CH $_2$ -CO), 2.08 (s, 3H, CH $_3$), MS(EI) m/z 217.50[M] $^+$,216.30 [M-H] $^+$ Anal. C 33.25; H, 3.26; N, 19.34

N'-benzoyl-2,4-dioxothiazolidine-3-carbohydrazide, (1n): FTIR (KBr) cm^{-1} 3017.30 (N-H str), 2985.6 (C-H aromatic str),

2196.20 (C-H aliphatic str), 1708.0 (CO-NHCO), 1643.8 (C=O str), 1528.2 (C=O str of amide), 1489.1(C-N aliphatic str), 889.0 (C-H aromatic bend), 684.0 (C-S str); ¹H NMR(400 MHz, DMSO-d₆, δ) 7.06 -7.25 (m, 7H, Ar-H&NH-NH of hydrazide); 3.81(s, 2H,S-CH₂-CO), MS(EI) m/z 277.20[M-2H]⁺, Anal. C, 47.30; H, 3.24; N, 15.06

N'-cinnamoyl-2, 4-dioxothiazolidine-3-carbohydrazide, (1o): FTIR (KBr) cm⁻¹ 3289.24 (N-H str), 2938.57 (C-H aromatic str), 2856.45 (C-H aliphatic str), 1789.24 (CO-NHCO) 1674.92 (C=O str), 1593.40 (C=O str of amide), 1490.90(C-N aliphatic str), 836.54 (C-H aromatic bend) 693.30 (C-S str); ¹H NMR(400 MHz, DMSO-d₆, δ) 8.0 (d, J=7.6Hz, 2H, NH-NH of hydrazide); 7.47-7.92 (m, 5H, Ar-H), 6.02 (d, 1H, NH), 6.89(d, J=15.6Hz, 1H, CH α =C), 4.12(s, 2H, S-CH₂-CO), MS(EI) m/z 305.1[M]⁺,304.3 [M-H]⁺Anal. C, 51.04; H, 3.61; N, 13.75

2, 4-dioxo-*N'*-(2-phenoxyacetyl)thiazolidine-3-carbohydrazide, (1p): FTIR (KBr) cm⁻¹ 3185.0 (N-H str), 2985.20 (C-H aromatic str), 2857.46 (C-H aliphatic str), 1729.50 (CO-NHCO) 1682.90 (C=O str), 1589.0 (C=O str of amide), 1573.23(C=C), 1476.0(C-N aliphatic str), 1226.30(C-O phenoxy str), 836.80(C-H aromatic bend 687.70 (C-S str); ¹H NMR(400 MHz, DMSO-d₆, δ) 8.40 (m, 1H, NH of hydrazide), 7.46-7.95 (m, 5H,Ar-H), 6.13 (d, 1H, NH of hydrazide) 4.60 (s, 2H, O-CH₂), 3.89(s, 2H,S-CH₂-CO), MS(EI) m/z 309.60[M]⁺,308.10 [M-H]⁺Anal. C, 46.45; H, 3.57; N, 13.58

N'-(octadec-9-enoyl)-2,4-dioxothiazolidine-3-carbohydrazide, (1q): FTIR (KBr) cm⁻¹ 3230.80 (N-H str), 2955.04 (C-H aromatic str), 2850.88 (C-H aliphatic str), 1739.85(CO-NHCO) 1629.90 (C=O str), 1599.04 (C=O str of amide), 1467.88(C-N aliphatic str), 1379.15(CH₂-bend), 1352.22 (CH₃-bend), 964.44 (C-H aromatic bend), 721.40 (C-S str); ¹H NMR(400 MHz, DMSO-d₆, δ) 8.89 (d, J=7.6Hz, 2H, NH-NH of hydrazide);), 5.32 (s, 2H, S-CH₂-CO), 4.03(t, 2H, CH₂-CO), 2.24-2.27(m,6H,olefinic& allylic , 1.21-1.99 (m,22H,CH₂), 0.89 (t, 3H, CH₃), MS(EI) m/z 439.80[M]⁺,438.00 [M-H]⁺Anal. C, 60.01; H, 8.47; N, 9.55

2, 4-dioxo-*N'*-palmitoylthiazolidine-3-carbohydrazide, (1r): FTIR (KBr) cm⁻¹ 3244.72 (N-H str), 2961.09 (C-H aromatic str), 2845.81 (C-H aliphatic str), 1733.77(CO-NHCO) 1632.86 (C=O str), 1592.12 (C=O str of amide), 1546.31(C=C), 1472.91(C-N aliphatic str), 1382.09(CH₂-bend), 1356.12 (CH₃-bend), 964.44 (C-H aromatic bend), 789.41 (C-S str); ¹H NMR (400 MHz, DMSO-d₆, δ), 8.57-8.76 (d, J=7.6Hz, 2H, NH-NH of hydrazide), 5.28 (s, 2H, S-CH₂-CO), 2.40 (t, 2H, CH₂-CO), 1.23-1.58 (m, 26H, CH₂),0.88 (t, 3H, CH₃), MS(EI) m/z 413.2[M]⁺,412.6 [M-H]⁺Anal. C, 58.19; H, 8.52; N, 10.15

2.2. In Vitro Cytotoxicity Studies MTT Assay

Michigan Cancer foundation (MCF-7) cancer cell lines were purchased from NCCS, Pune. MTT assay was performed with five concentrations of compounds in triplicates. The optical density was measured at 570 nm on a

micro plate reader. The IC₅₀ values of the studied compounds were calculated from the concentration response curves generated using Graph Pad prism 7.0 Software [15].

2.3. *In Vitro* Monoacylglycerol Lipase (MAGL) Inhibition Assay

MAGL inhibition leads to a reduction of free fatty acids (FFAs) and lysophosphatidic acid (LPA), and thereby attenuate cancer cell pathogenicity. MAGL inhibition assay was performed using kit commercially obtained Cayman (kit no 705192). In brief reaction mixture consist of 150µl of assay buffer (Ix), 10µl of test compounds, JZL 195 provided along with the kit was used as the positive control. The reaction mixture was incubated for 10 min at room temperature, and absorbance was read at 405-415nm.

$$\% \text{ Inhibition} = \frac{(\text{Initial activity (IA)} - \text{Inhibitor/Initial activity})}{\text{Initial activity}} * 100$$

The IC₅₀ values for the selected compounds which showed more than 50% inhibition at 50µM concentration were calculated from the concentration response curves generated using Graph Pad prism 7.0 Software [16].

2.4. *In Silico* Studies

2.4.1. *Molecular Docking Studies*

Chemical structures of the azaglycinamides were drawn using Chem & Bio Draw 12.0, saved as mol2 files using Chem & Bio 3D version 12.0. Chemical structures were optimized using Flare, a software by Cresset [17, 18] Crystal structure of bovine Cathepsin B in complex with NS-134, a two-headed

epoxysuccinyl inhibitor (PDB ID: 1SP4) and the crystal structure of a soluble form of human monoglyceride lipase in complex with an inhibitor, ZYH ((2-cyclohexyl-1,3-benzoxazol-6-yl){3-[4-(pyrimidin-2-yl)piperazin-1-yl]azetid-1-yl}methanone) (PDB ID: 3PE6), were used for the molecular docking studies. As the targets possessed inbuilt ligands NS-134, and ZYH, the active sites for the same have been considered to explore the binding affinities of the synthesized compounds. Protein structures were minimized using Flare tool v 2.0 (Cresset, Lillington, Cambridge shire, UK; (<http://www.cresset-group.com/flare/>)). The grid box was defined around the crystal inhibitor of downloaded target structures. The docking process was accomplished using normal mode and default settings of the software. Electrostatic complementarity (EC) maps were based on a calculation of electrostatic potentials for the ligand and the protein on the ligands surface. Electrostatic potentials are summed together, normalized, and then scaled. Green colored regions indicate perfect electrostatic complementarity with the protein, while red color suggests that there is a perfect electrostatic clash at the site. N-1834 and JZL-195 were used as reference compounds to compare the docking results in molecular docking with cathepsin B and MAGL, respectively (Table 3, 4).

2.5. *Pharmacological Studies*

2.5.1. *Animals Used*

Animal care and handling were carried out according to the ethical guidelines set by the

Committee for the purpose of Control and Supervision on Experimentation of Animals (CPCSEA). The Institutional Animal Ethical Committee had approved all the animal experimental protocols (CPCSEA 1677/PO/Re/S/2012/IAEC/04 Dt. 27-04-17). Animals were fasted before dosing for 4hrs with water *ad libitum*.

2.5.2. Methods

2.5.2.1. Acute Oral Toxicity Studies

The concepts of the up-and-down testing approach (UDP) were followed to determine the acute toxicity of chemicals as per OECD guidelines 425. The dose of 175 mg/kg was considered as sublethal and used to evaluate therapeutic activity for the reduction of pain [19]. Hence, in the present study this dose was selected as the starting dose.

After dosing every 30 minutes individual animals were observed for 4h, intermittently for 24 h and daily after that for a total of 14 days for mortality. Gross behavioral changes, tremors, convulsions, salivation, diarrhea, lethargy, and sleep were observed during 24 h. If the previously tested animal was found safe then the next concentration level was given to the animals.

2.5.2.2. Eddy's Hot Plate Method

Mice were placed on a hot plate ($56^{\circ}\pm 1^{\circ}\text{C}$) and thermal stimulus was applied. Centrally acting analgesics increase the latency to lick the paws or jump from the hot plate [20]. Male mice weighing 25-30 g were divided into different groups of six each. Group I serves as

vehicle control, group II was given standard (tramadol 10 mg/kg, p.o), remaining groups were treated with test compounds (55 mg/kg, p.o). The response latency (time taken for jumping from the hot plate) was recorded after 1 hr after administration of the test and standard compounds. To prevent tissue damage the test was terminated at 15 seconds.

2.5.2.3. Tail Immersion Method

This method is widely used to screen centrally acting analgesic agents. Mice were divided into different groups, control, standard, and test (6 animals per group). The mice were gently wrapped in a cloth, and the latency in seconds for withdrawal of tail immersed in warm water maintained at $55\pm 1^{\circ}\text{C}$ was recorded, after oral administration of the test (55 mg/kg, p.o) and standard compounds (tramadol 10 mg/kg, p.o). The cut off time was 15 sec, to avoid tissue injury [21].

2.5.2.4. Allyl Isothiocyanate (AITC) Induced Nociception Method

Transient receptor potential ankyrin 1 (TRPA1), activation evokes nociception via the release of substance P. AITC induced nociceptive behaviors (licking and flinching of injected paw, measured in seconds in hind paw) were assessed up to 5 min [22].

Mice were divided into different groups (n=6), six for each. Control animals received an equivalent amount of vehicle solutions. One hour after administering the test (55 mg/kg, p.o) and standard doses (diclofenac 50 mg/kg p.o), 0.05 ml of 1% solution of AITC was injected

into the left hind paw of each mouse. The numbers of lickings or flinchings were measured after 15 min following AITC injection, individually for 5 min.

2.5.2.5. Statistical Analysis

Data from the *in vivo* studies was expressed as mean \pm standard error of mean (SEM) of 6 observations, and evaluated by using One – way analysis of variance (ANOVA) followed by Turkey's multiple comparison test by using Graph pad Prism Software version 7.0 (Graph pad software, Inc. La Jolla, CA, USA). The confidence level of $p < 0.05$ was considered statistically significant.

3. Results and Discussion

3.1. Chemistry

A series of pyrrolyl, imidazolyl, and thiazolidine 2, 4-dione substituted azaglycinamides (**1a-1r**) was synthesized as depicted in [scheme I](#). The methodology involves pyrrole/imidazole/thiazolidine 2, 4-dione, and various substituted hydrazides as building blocks. The heterocyclic azaglycinamides were readily obtained by treating the desired heterocyclic ring with ethyl chloroformate in triethylamine to form the corresponding reactive ethyl carbamate intermediates. These intermediates were subsequently reacted with various substituted hydrazides (acetyl, benzoyl, cinnamoyl, phenoxy acetyl, oleoyl, and palmitoyl) to obtain the title compounds ([Table 1](#)).

The compounds were purified by recrystallization (ethanol) and column

chromatography (Chloroform: ethyl acetate: 1:2). The methodology is considered highly amenable and an efficient method for amide bond formations. Couplings reactions were performed in inert dry solvents, in the presence of a non nucleophilic base viz triethylamine or N-methyl morpholine (NMM), to trap the formed hydrochloric acid. The versatility of this amide bond formation methodology was supported by Sun et al., who reported this approach for the synthesis of various carboxamides [23]. The compounds were obtained in good yields, and the purity of the compounds was characterized by spectral analysis using FTIR, ^1H NMR, and Mass spectroscopy. FT-IR spectra of the compounds displayed characteristic absorption peaks in the region of 3400-3300 cm^{-1} due to N-H, 2950-2900 cm^{-1} due to aromatic stretchings, 1680-1600 cm^{-1} due to carbonyl amide stretchings. ^1H NMR (400 MHz, DMSO- d_6 , δ ppm) displayed multiplets from 3.8-4.5 due to $\text{CH}_2\text{-N}$, multiplets in the region of 7.0-8.3 due to aromatic protons, doublets between 8.4-8.8 due to hydrazide protons. The imidazole C-H proton showed singlets in the region of 9.0-9.4. The absence of a peak at δ 12.35-12.45 ppm showed the involvement of NH of thiazolidine-2, 4-dione in amide bond formation, and confirms the formation of title products. The results evidenced from the ^1H NMR analysis for the observation of no peaks in the region of δ 12.02 ppm, which are characteristic for the secondary amine, NH of thiazolidine are following the results reported by Pinheiro et al [24]. The compounds exhibited (M-H) $^+$ peaks as the molecular ion peaks for most of the

compounds at their characteristic m/z values. The observation of the $(M-H)^+$ peak as the molecular ion peak might be because the N-H proton readily breaks, and the major fragmentation pattern involved the cleavage at the aza linkage $-NH-NH-$ as reported by Gray et al. [25].

3.2. In Vitro Activity

3.2.1. Cytotoxicity Studies

All the compounds were evaluated for cytotoxicity on the MCF-7 cell line by MTT assay. The concentration of the test samples (**1a-1r**) and the anticancer agent Cisplatin that induced 50% inhibition (IC_{50}) in malignant MCF-7 cell survival was determined (Table 2). Out of eighteen compounds, nine compounds (**1d**, **1e**, **1f**, **1j**, **1k**, **1l**, **1p**, **1q**, and **1r**) were active with IC_{50} values in the range of 41.13-61.10 μ M, whereas other compounds showed moderate to low cytotoxicity. N-oleoyl and N-palmitoyl functionalized azaglycinamides were the most potent among the synthesized compounds suggesting the importance of lipophilicity and steric bulk of N-functionalization for cytotoxicity. The N-oleoyl functionalized azaglycinamides **1e**, **1k**, and **1q** (IC_{50} values 54.19, 57.72 & 41.13 μ M respectively) have shown almost fivefold cytotoxicity as compared to the N-acetyl azaglycinamides and two-fold cytotoxicity as compared to the N-phenoxy acetyl azaglycinamides. Next in the cytotoxic potency line were the N-palmitoylated derivatives **1f**, **1l**, and **1r** with IC_{50} values of 58.72, 61.10 & 49.80 μ M, respectively. However, the potency was

less than that of standard drug Cisplatin (IC_{50} 4.4 μ M). A perusal of the data also indicates that thiazolidine-2, 4-dione containing derivatives (**1q** & **1r**) were more potent than C-pyrrolyl and C-imidazolyl counterparts. The effect of C-functionalization revealed that the most active compounds in this series were those with C-functionalized thiazolidine-2, 4-dione moieties. Our observations demonstrated that the compound **1q** which possess thiazolidine 2, 4-dione moiety on the carboxylic group of azaglycinyl scaffold, showed highest cytotoxic profile with IC_{50} value of 41.13 μ M towards the MCF-7 cell lines than their C-pyrrolyl functionalized (**1e**, 54.19 μ M) and imidazolyl (**1k**, 57.72 μ M) counterparts.

The study aimed to focus on the importance of the acyl chain on the amino group of azaglycine moiety (N-functionalization) and amide derivative of the carboxyl moiety with various heterocycles (C-functionalization). The noticeable activity of compounds **1q** and **1r** might be due to the lipophilic side chain, which may increase cell membrane permeability and cytotoxic activity. The results are well accorded by the observations emphasized by Lbachir et al. and the broad spectrum of activities including cytolytic, antiviral, and antifungal activities of lipopeptides, which were predictable due to the lipophilic tail that can compensate for the hydrophobicity and amphipathic structure of the peptide chain [26]. These results provide an intuitive sense that N-oleoylation and palmitoylation impart hydrophobicity and increase cell membrane permeability due to their lipophilic tails, hence

displaying cytotoxic activity against the MCF-7 cell lines. The biological activities associated with thiazolidine derivatives are attributed to its tendency to cause the inhibition of macrophages, suppression of inflammatory molecules such as interleukins (IL-1 and IL-6), tumor necrosis factor (TNF), and induced nitric oxide synthase (INOS) [27].

This privileged N- and C-functionalization approach of azaglycine implicates that N-oleoyl and C- thiazolidine- 2, 4-dione functionalized azaglycyl modification serves to be the most significant for the cytotoxic profile of azaglycinamides.

3.2.2. Monoacylglycerol Lipase (MAGL) Inhibition Studies

MAGL, a membrane-associated serine hydrolase that catalyzes the lipolytic cascade's final step responsible for releasing fatty acids from triacylglycerol, is considered a novel target for the treatment of pain, neuroinflammatory disorders, and cancer [28].

The *in vitro* MAGL inhibition assay revealed that most of the synthesized compounds were found to possess inhibitory activities varying from moderate to low active at 50 μ M concentrations (Table 2). The N-acetyl azaglycinamides, functionalized with either pyrrolyl or imidazolyl or thiazolidine - 2, 4-dione moieties (1a, 1g & 1m) showed low inhibition of MAGL as reflected from the low inhibitory potentials at 50 μ M. The N-benzoyl and N-cinnamoyl functionalized derivatives (1b, 1c, 1h, 1i, 1n, and 1o) showed moderate inhibition and the N- phenoxy acetyl

substituted derivatives showed good inhibition of MAGL 32 % (1d), 17.92% (1j) and 38.76% (1p). An examination of the effects of C-functionalization led us to interpret that substitutions with thiazolidine 2, 4-dione are more encouraging than the pyrrolyl, which are more favorable than imidazolyl scaffolds. Compound 1q (N-oleoyl, thiazolidine 2, 4-dione containing azaglycinamide) was active among the compounds tested in the series achieving an inhibition level of 72.34 % at 50 μ M. IC₅₀ values were determined for those compounds, which showed more than 50 % inhibition at 50 μ M (Table 3). A perusal of the data revealed apparent effective inhibitory potency (IC₅₀ 21.05 μ M) of the N-oleoyl azaglycinamide with thiazolidine 2, 4-dione functionalization. However, the potency was less than that for standard, JZL-195, IC₅₀ value of 2.01 μ M

Compounds 1e, 1k, and 1q bearing the N-oleoyl functionalization and pyrrolyl, imidazolyl or thiazolidine -2, 4-dione functionalization on the azaglycine scaffold proved to have interesting *in vitro* MAGL inhibition activities, giving a clear-cut indication regarding the biological significance of N-oleoyl substitution.

In the present study, it was observed that azaglycinamides have the potential to inhibit the MAGL enzyme. Several reversible (pristimerin, euphol, and octhilinone) and irreversible (JZL 184, OMDM169, and NAM) inhibitors were developed for MAGL, targeting either catalytic serine residue or any one of the Cys residues present near the active site.

Moreover, JZL-184 and OMDM169 are selective MAGL inhibitors and demonstrated antinociceptive activities [29]. The significant activity of the thiazolidine 2, 4-dione functionalized N-oleoyl azaglycinamide might be attributed to their structural resemblance to maleimides featuring nitrogen-containing five-membered dione as MAGL inhibitors [30]. The *in vitro* cytotoxicity and MAGL assay results signify the potentiality of azaglycinamides for anticancer and antinociceptive activities.

3.3. Molecular Docking Studies

3.3.1. Molecular Docking Studies on Cathepsin B (PDB ID 1SP4)

The breast carcinoma cell lines, MCF-7, are characterized by the localization of cathepsin B, an intracellular lysosomal cysteine protease involved in the degradation and processing of proteins, inflammatory responses against antigens, tissue modeling, and apoptosis [31]. Cathepsin B has been implicated in the initiation, promotion, and dissemination of cancers, including inflammatory breast cancer (IBC) [32]. The predominant expression of the cathepsin B renders this enzyme the primary target for developing novel drugs as anticancer agents [33].

The molecular docking studies on cathepsin B (PDB ID: 1SP4) indicated that most of the derivatives were found to bind with loop region amino acids like His-110, Gly-121, and Glu-122. The lowest binding affinity was observed for N-acetyl derivatives, followed by moderate binding affinities of N-benzoyl, N-cinnamoyl, and N- phenoxy acetyl derivatives and highest for N-oleoyl and palmitoyl derivatives (Table

3). The results showed that there is a correlation between *in vitro* efficiency and docking pattern. Compounds **Iq** (N-oleoyl) and **Ir** (N-palmitoyl) showed good binding affinity for Cathepsin B with -11.83 and -11.77 kcal/mol, respectively.

The overlay of 1q, 1r, NS-134, and N-1845 showed that they have similar binding patterns at the binding site (Figure 7). For the rest of the compounds, binding poses were slightly different due to the N-functionalized variations. 1q, the most active compound in the docking studies, showed one hydrogen bonding (CO group with ring hydrogen of His-110) and one van der Waals interaction (-CH₂- of oleoyl chain with the carbonyl group of Gly-198), while 1r showed three hydrogen bonding interactions (CO group with ring hydrogen of His 110 and with the hydrogen of Gln-23; CO of 2,4-thiazolidinedione with ring hydrogen of Trp-221) and one van der Waals interaction (CO of 2,4-thiazolidinedione with ring hydrogen of His-199). For NS-134, a covalent inhibitor of cathepsin B, hydrogen bonding interactions were observed with His- 110 and His-111 and van der Waals interactions with Cys-29 (Figure 8). Most of the compounds mimicked the covalent inhibitor and azaglycinyl derivative N-1845 in their binding interactions. Length of the N-substitution and flexibility played a significant role in molecular docking studies with Cathepsin B and MAGL enzymes.

The data clearly shows that the carbonyl oxygen and the aza nitrogen atoms of the azalinkage (-CO-NH-NH-CO-) are involved in the hydrogen bonding with Cys-26, Gln-23,

Gly-121, Glu-122 amino acids, which are the critical amino acids in the binding pocket of 1SP4. These results are well supported by Izabela et al., where the carbonyl group of the built in ligand also formed hydrogen bonding with the critical amino acid Cys-29[34]. N-palmitoyl, N-oleoyl, and N-phenoxy acetyl functionalized azaglycinamides exhibited interactions with target enzymes. These observations suggest that the binding pocket of cathepsin B can accommodate bulky substituents, favoring good binding with the target enzyme. C-functionalization with heterocyclic moiety also contributed to the binding and 2, 4-thiazolidinedione was more favorable than imidazole and pyrazole rings. Electrostatic complementarity was found to be good in all N-oleoyl and palmitoyl derivatives (Figure 6). The results are in agreement with the previous reports by Wieczerszak et al. stating that azaglycine incorporated azapeptides at the N-terminus were proved to be highly potent and selective inhibitors of cathepsin B ($K_i=0.088\text{nM}$), than their conserved glycine derivatives [35].

3.3.2. Molecular Docking Studies on Monoacylglycerol Lipase (PDB ID 3PE6)

The molecular docking studies on MAGL (PDB ID: 3PE6) revealed the binding affinities in the order of N-acetyl < benzoyl < phenoxy acetyl < cinnamoyl < palmitoyl < oleoyl, indicating that presence of long-chain fatty acid acyl chain favors good binding to the target enzyme (Table 4). The highest binding affinities were displayed by N-oleoyl

thiazolidine 2, 4-dione followed by N-oleoyl imidazolyl and N-oleoyl pyrrolyl derivatives (**1q**, **1e**, and **1k**, -14.82, -13.50 & -13.39 kcal/mol) better than the standard JZL 195 (-13.09 kcal/mol). The compounds 1q, 1e & 1k with the highest binding affinities were found to display hydrogen bonding between the carbonyl oxygens, aza nitrogen of the azaglycynyl moiety, and Arg-57, Tyr-94, Glu-53 in the active site of the enzyme (Figure 9, Figure 10, and Figure 11)

The validation of the method was performed by submitting the built-in ligand for docking. As per the binding interactions, the ligand oxygen was involved in hydrogen bonding with Met-123 NH. These results were in accordance with the predicted observations, as reported by Celine et al. [36]. Preferred binding poses of the docked compounds and JZL-195 were similar, whereas the co-crystallized ligand's binding pose, ZYH, was different, which showed interactions with Ser-122, Met-123, Ala-5, and Tyr-194. A good correlation was observed between *in vitro* cytotoxicity, MAGL inhibition, and molecular docking studies with these derivatives. The docking results corroborate with *in vitro* MAGL inhibition assay and are also supported by the observation made by Matuzak et al. [30], where N-oleoyl substituted maleimides possessed good *in vitro* inhibition of MAGL. As observed in the case of the docking results of cathepsin B, these compounds also showed the involvement of the carbonyl oxygen and the aza nitrogen of the aza moiety in the binding of the critical amino acids. These results suggest the role of the aza moiety in enhancing the binding interactions

due to the additional hydrogen bonding capability of the NH group, supported by Zhang et al. [37].

3.4. Anti Nociceptive Studies

3.4.1. Acute Toxicity Studies

In our study, test compounds were found to be safe up to 550 mg/kg, p.o, with no signs of mortality and gross behavioral studies. Hence, a test dose of 55 mg/kg, p.o, was used to evaluate the *in vivo* antinociceptive effect of the synthesized compounds. Compounds **1e**, **1k** & **1q**, which showed good *in vitro* MAGL inhibitory activity, were selected for *in vivo* antinociceptive screening assays.

3.4.2. Eddy's Hot Plate Method

Our findings demonstrated that azaglycinamides bearing C-functionalized thiazolidine 2, 4-dione, **1q** and pyrrolyl moiety, **1e** exhibited a significant increase of latency time to pain reaction compared to the control group (Table 5). The imidazolyl functionalized N-oleoyl azaglycinamide, **1k** showed moderate activity. A perusal of the results suggests that the features of C-functionalization with thiazolidine-2, 4-dione and N-oleoyl functionalization might significantly influence the attenuation of pain responses elicited by thermal hyperalgesia. The results are in accordance with the thiazolidine moiety's potentiality in anti-inflammatory response, as reported by Laudelina et al. [38]. These results indicated that thiazolidine-2,4-dione analogs might possess antinociceptive activity by

reducing mediators' synthesis involved in the nociceptive responses [39].

3.4.3. Tail Immersion Method

The results were recorded as the average of the reaction time of withdrawal of the tail or jerk of tail with a cut off time of 15 s. Gross observations of the results revealed that mice treated with **1q** showed a statistically significant reduction of pain reactivity threshold than those treated with either **1k** or **1e**. However, the analgesic activity of these derivatives was less significant than standard tramadol (10 mg/kg). The results implicate that substitution of a large lipophilic group (N-oleoyl) and C-thiazolidine 2, 4-dione functionalization favors analgesic potentiality of azaglycine moiety via the central mechanism.

3.4.4. Allyl Isothiocyanate (AITC)-Induced Nociception

Allyl isothiocyanate (AITC) is a transient receptor potential ankyrin (TRPA1) agonist which induces inflammatory edema in a COX (cyclooxygenase) dependent manner. The reduction in the nociceptive behavioral responses like the licking of the injected paw/number of flinching responses is considered to assess the antinociceptive activity in this model. Significant antinociceptive activity was observed for **1q**, when compared to control, which displayed (23.33±0.48)/5 min, lickings, and (20.83±0.48)/5 min, flinchings. The decrease in the number of licking and flinching responses for these derivatives was

less in comparison with a standard (diclofenac, 50 mg/kg, p.o). The number of lickings was $(17.17 \pm 0.40)/5$ min for **1q**. Effect of title compounds in hot plate, tail immersion, and AITC methods were tabulated in Table 5.

The test compounds attenuated pain responses related to neurogenic inflammation elicited by allyl isothiocyanate by reducing the number of nocifensive responses. Compound **1q** antagonized these nocifensive responses comparable to the standard diclofenac at 50 mg/kg, p.o giving an intuitive sense that this derivative could be a potential novel analgesic for acute and neuropathic pain. Thus **1q** could be considered as effective in blocking pain behaviors induced by inflammation, similar to the findings by Boonen et al. [40].

4. Conclusion

In conclusion, our attempts to study the influence of N- and C- functionalization with the varied chain lengths and varied heterocyclic moieties on azaglycyl scaffold suggest that, long chain fatty acyl substitutions such as N-oleoyl and N-palmitoyl functionality and the C-functionalization with 2, 4-thiazolidinedione scaffold seems determinant for MAGL enzyme inhibition. The synthesized amide derivatives of azaglycine with core N-oleoyl and C-thiazolidine-2, 4-dione functionalization could be the lead molecules to exemplify the various biological activities. Though most of the title compounds have shown moderate activity, this kind of N & C-functionalization of azaglycine with other structural variants can be focused on the development of new therapeutic agents.

Acknowledgements

The authors are thankful to SPMVV and Cresset, Lillington, Cambridge shire, UK; (<http://www.cresset-group.com/flare/>).

References

- [1] Gao J. Recent Advances in Peptide Immuno Modulators. *Curr. Top Med. Chem.* (2015)187-205.
- [2] Avan I, Hall CD and Katritzky AR. Peptidomimetics via Modifications of Amino acids and Peptide Bonds. *Chem. Soc. Rev.* (2014)43:3575-3594.
- [3] Zega A. Azapeptides as Pharmacological Agents. *Curr. Med. Chem.* (2004)12:589-597.
- [4] Lv Z, Chu Y and Wang Y. HIV Protease Inhibitors: A Review of Molecular Selectivity and Toxicity. *HIV/AIDS – Res. Palliat. Care.* (2015)95–104.
- [5] Kurian LA, Silva T A and Sabatino D Submonomer Synthesis of Azapeptide Ligands of the Insulin Receptor Tyrosine Kinase Domain. *Bioorg. Med.Chem. Lett.* (2014)24:4176-4180.
- [6] Loser R, Frizler M, Schilling K and Gutschow M. Azadipeptide Nitriles: Highly Potent and Proteolytically Stable Inhibitors of Papain-like Cysteine Proteases. *Chem. Int. Ed.* (2008) 47:4331-4334.
- [7] Dinh TP, Carpenter D, Leslie FM, Freund TF, Katona I and Sensi SL. Brain Monoglyceride Lipase Participating in Endocannabinoid Inactivation. *Proc. Natl. Acad. sci. USA* (2002)99:10819-10824.
- [8] Alpizar YA, Gees M, Sanchez A, Apetrei A, Voets T, Nilius Band Talavera K. Bimodal Effects of Cinnamaldehyde and Camphor on Mouse TRPA1. *Pflug. Archiv.* (2013)465:853–864.
- [9] Walter H. New Carboxylic Acid Amides of the Pyrrole Series: Synthetic Routes and Biological Aspects. *Z. Naturforsch.* (2008) 63:351 – 362.
- [10] Petit S, Fruit CandBischoff L. New Family of Peptidomimetics Based on the Imidazole Motif. *Org. Lett.* (2010)12:4928-4931.

- [11] Apotrosoaei M, Vasincu I, Constantin S, Buron F, Routier S and Profire L. Synthesis, Characterization and Antioxidant Activity of Some New Thiazolidin-4-one Derivatives. *Rev. Med. Chir. Soc. Med. Nat. Iasi.* (2014)18:213-218.
- [12] Carpenter CA, Kenar JA and Price NPJ. Preparation of Saturated and Unsaturated Fatty Acid Hydrazides and Long Chian C-glycoside ketohydrazones. *Green Chem.* (2020)12:2012-2018.
- [13] Celine S. Crystal Structure of a Soluble form of Human Monoglycerol Lipase in Complex with an Inhibitor at 1.35 Å resolution *Protein sci.* (2011)20:670-683.
- [14] Prashanthi G, Prasad KVSRRG and Bharathi K. Design, Synthesis and Evaluation of dialkyl 4-(benzo[d][1,3]dioxol-6-yl)-1,4-dihydro-2,6-dimethyl-1-substitutedpyridine-3,5-dicarboxylates as Potential Anticonvulsants and their Molecular Properties Prediction. *Eur.J.Med.Chem.* (2013)66:516.
- [15] Eddy NB and Leimbach D. Synthetic Analgesic II. Dithienylbutenyl and Dithienylbutylamines. *J. Pharmacol. Exp. Ther.* (1953)107:385–393.
- [16] Muccioli GG, Geoffrey Labar and Lambert MD. CAY10499, A Novel Monoglyceride Lipase Inhibitor Evidenced by an Expeditious MGL Assay. *Chem. Bio. Chem.* (2008)9:2704-2710.
- [17] Cheese right T, Mackey M, Rose S and Vinter A. Molecular Field Extrema as Descriptors of Biological Activity: Definition and Validation. *J. Chem. Inf. Model.* (2006) 46:665–676.
- [18] Score VS. Docking Factor-Xa ligands with Lead Finder- Case Study. *T. C. a. f. u. software* [online] (2016). Available from: <https://www.cresset-group.com/tag/lead-finder>.
- [19] Dixon WJ. Staircase Bioassay: The Up -and-Down Method. *Neurosci. Biobehav. Rev.* (1995)15:47-50.
- [20] Haseena banu B, Prasad KVSRRG and Bharathi K. Synthesis and Biological Evaluation of N-dehydrodipeptidyl-N,N'-dicyclohexylurea Analogs. *Eur. J. Med. Chem.* (2014)78:72-85.
- [21] Rajitha G, Prasad KandBharathi K. Synthesis and Biological Evaluation of 3-Amino Pyrazolones. *Asian J. Chem.* (2011)23:684-686.
- [22] Nakamura Y, Une Y, Miyano K, Abe H, Hisaoka K, Morioka N and Nakata Y. Activation of Transient Receptor Potential Ankyrin 1 Evokes Nociception through Substance P Release from Primary Sensory Neurons. *J. Neurochem.* (2012)120:1036-1047.
- [23] Sun. 4-(2-Pyridyl) piperazine-1-carboxamides: Potent Vanilloid Receptor 1 Antagonists. *Bioorg. Med. Chem. Lett.* (2003)13:3611–3616.
- [24] Pinheiro DS, Junior ENS and Consolini G. Optimized Synthesis and Characterization of Thiazolidine-2, 4-dione for Pharmaceutical Application. *J. Biorg. Org. Chem.* (2017)1:122–126.
- [25] Gray MD, Jeschsa SA and Stein GH. 5-Azacytidine-Induced Demethylation of DNA to Senescent Level does not Block Proliferation of Human Fibroblasts. *J. Cell. Physiol.* (1991)8:477-484.
- [26] Lbachir Ben Mohamed, Radhika Krishnan, Catherine Auge, James F. P and Don J D Intranasal Administration of a Synthetic Lipopeptide Without Adjuvant Induces Systemic Immune Responses, *Immunology* (2002)106:113–121.
- [27] Mishra G, Sachan N and Chawla P. Synthesis and Evaluation of Thiazolidinedione–Coumarin Adducts as Antidiabetic, Anti–Inflammatory and Antioxidant Agents. *Letter in Org. Chem.* (2015)12:429–445.
- [28] Matej Sovaeljkoak, Jelena A, Samo Turk, Zorica DJ and Irena Mlinari Rascan Stanislav Gobec. Cinnamic Acid Derivatives Induce Cell Cycle Arrest in Carcinoma Cell Lines. *Med. Chem.* (2013) 11:9-15.
- [29] Rea P, Jatta T, Olli E, Francisco RLP, Merja H and Juha OR. Monoacylglycerol Lipase Inhibitor JZL184 Reduces Neuroinflammatory Response in APdE9 Mice and in Adult Mouse Glial Cells. *J. Neuroinflam.* (2015) 12:81- 92.
- [30] Matuzak N, Giulio G, Muccioli, Geoffrey Labar and Lambert MD. Synthesis and in Vitro Evaluation of N-Substituted Maleimide Derivatives as

Selective Monoglyceride Lipase Inhibitors. *J. Med. Chem.* (2009) 52:7410–7420.

[31] Levenson AS and Jordan VC. MCF-7: The First Hormone-Responsive Breast Cancer Cell Line. *Cancer Res.* (1997) 57:3071-3078.

[32] Mohamed MM and Sloane BF. Cysteine cathepsins: Multifunctional Enzymes in Cancer. *Nat. Rev. Cancer.* (2006) 6:764-775.

[33] Zhou Z, Wang Y and Bryant SH. Multi-conformation 3D QSAR Study of Benzenesulfonyl-Pyrazol-ester Compounds and their Analogs as Cathepsin B Inhibitors. *J. Mol.Graph.Model.* (2011) 30:135-147.

[34] Izabela P and Bonnie FS. Cathepsin B and its role in Cancer Progression. *Biochem. Soc. Symp.* (2003)70:263-276.

[35] Wiczerzak E, Jamkowska S, Rodziewicz-Motowidlo A, Gieldon J, Lagiewka Z, Grzonka M, Abrahamson A, Grubb A and Bromme D. Novel Azapeptide Inhibitors of Cathepsins B and K.

Structural Background to Increased Specificity for Cathepsin B. *The J. Pept. Res.* (2005) 66:1–11.

[36] Celine SH. Crystal Structure of a Soluble form of Human Monoglycerol Lipase in Complex with an Inhibitor at 1.35 Å resolution. *Protein sci.* (2011) 20:670-683.

[37] Zhang Y, Malamakal RM and Chenoweth DM. Aza-Glycine Induces Collagen Hyperstability. *J. Am. Chem. Soc.* (2015)137:12422-12425.

[38] Laudelina RM. Activity Anti-Inflammatory and in silico Study of New Thiazolidinedione Derivatives. *Brit. J. Pharm. Res.* (2014) 4:1739-1752.

[39] Wongmayura A and Songkram C. (eds.) Synthesis and COX inhibitory activity of thiazole analogs derived from classical NSAIDs. *Proceedings of the 6th Regional IMT-GT Uninet, Penang;* (2008) Aug28-30; Malaysia.

[40] Brett Boonen, Justyna BS and Karel Talavera. Chemical Activation of Sensory TRP Channels. *Topics in Med. Chem.* New York Springer, (2016) 23:73–113.

Tables:

Table 1. Physical data of Pyrrolyl, Imidazolyl azaglycinamides (1a-1l) and thiazolidine - 2, 4-dione azaglycinamides (1m-1r).

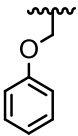
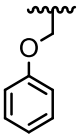
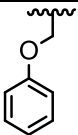
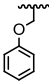
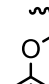
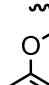
Compound	R	X	Molecular formula	% Yield	Melting point
1a	CH ₃	CH	C ₇ H ₉ N ₃ O ₂	60	206-209
1b	C ₆ H ₅	CH	C ₁₂ H ₁₁ N ₃ O ₂	70	211-218
1c	C ₆ H ₄ CH=CH	CH	C ₁₄ H ₁₃ N ₃ O ₂	70	205-209
1d		CH	C ₁₃ H ₁₃ N ₃ O ₃	55	229-232
1e	Oleyl	CH	C ₂₃ H ₃₉ N ₃ O ₂	50	216-218
1f	palmityl	CH	C ₂₁ H ₃₇ N ₃ O ₂	55	195-198
1g	CH ₃	N	C ₆ H ₈ N ₄ O ₂	65	200-202
1h	C ₆ H ₅	N	C ₁₁ H ₁₀ N ₄ O ₂	60	216-220
1i	C ₆ H ₄ CH=CH	N	C ₁₃ H ₁₂ N ₄ O ₂	55	235-240
1j		N	C ₁₂ H ₁₂ N ₄ O ₃	55	210-213
1k	Oleyl	N	C ₂₂ H ₃₈ N ₄ O ₂	40	122-125
1l	palmityl	N	C ₂₀ H ₃₆ N ₄ O ₂	40	208-212
1m	CH ₃	-	C ₁₆ H ₇ N ₃ O ₄ S	60	158-160
1n	C ₆ H ₅	-	C ₁₁ H ₉ N ₃ O ₄ S	75	96-98
1o	C ₆ H ₄ CH=CH	-	C ₁₃ H ₁₁ N ₃ O ₄ S	70	79-84
1p		-	C ₁₂ H ₁₁ N ₃ O ₅ S	60	112-115
1q	Oleyl	-	C ₂₂ H ₃₇ N ₃ O ₄ S	50	112-114
1r	palmityl	-	C ₂₀ H ₃₅ N ₃ O ₄ S	55	167-170

Table 2. *In vitro* cytotoxicity and MAGL inhibition of the synthesized functionalized azaglycinamides.

Compound	R	Cytotoxicity studies		<i>In vitro</i> MAGL inhibition	
		IC ₅₀ Values μM ^a	% Inhibition at 50 μM ^a	IC ₅₀ Values μM ^b	
1a	CH ₃	162.31±9.20	7.41±0.82	---	
1b	C ₆ H ₅	156.80±6.40	9.01±1.10	---	
1c	C ₆ H ₄ CH=CH	187.40±11.20	9.91±0.67	---	
1d		67.24±4.20	32.00±2.12	---	
1e	Oleyl	54.19±3.60	52.61±3.40	51.12±2.92	
1f	palmityl	58.72±2.80	48.11±1.8	---	
1g	CH ₃	189.71±10.10	5.28±1.10	---	
1h	C ₆ H ₅	88.39±5.40	19.90±0.90	---	
1i	C ₆ H ₄ CH=CH	191.48±10.80	16.21±0.87	---	
1j		74.32±3.70	17.92±1.10	---	
1k	Oleyl	57.72±2.40	62.21±0.89	42.97±3.60	
1l	palmityl	61.10±3.20	36.76±0.92	---	
1m	CH ₃	152±9.60	17.91±1.10	---	
1n	C ₆ H ₅	123±6.40	19.23±1.60	---	
1o	C ₆ H ₄ CH=CH	134±7.20	20.16±2.10	---	
1p		65.41±3.64	38.76±1.60	---	
1q	Oleyl	41.13±2.68	72.34±2.10	21.05±1.20	
1r	palmityl	49.80±3.10	46.76±3.60	---	
Standard	Cisplatin	4.4±0.70	(JZL 195) 89.96±7.30	2.01±0.60	

All the values presented were mean ± SEM from three independent observations. a. The compounds which showed more than 50% inhibition at 50 μM concentration were further selected for IC₅₀ calculations in MAGL inhibition assay. b. Hydrolysis of 4-nitrophenylacetate results in formation of yellow product which shows absorbance between 405-412 nm.

Table 3. Molecular docking of the synthesized functionalized azaglycinamides on Cathepsin B.

Compound	LF VS Score (kcal/mol)	Interacting amino acids	Type of interactions	Bond distance
1a	5.25	His-110	Hydrogen bonding	1.9
1b	6.35	His-110	Hydrogen bonding	2.1
		His-199	Aromatic-Aromatic	3.6
1c	5.82	Cys-29	Hydrogen bonding	2.3
		Gln-23	Hydrogen bonding	2.3
1d	7.04	Glu-122	Hydrogen bonding	2.0
1e	9.97	His-110	Hydrogen bonding	1.9
1f	9.10	His-111	Hydrogen bonding	2.2
		Cys-119	Sulphur-Lonepair	4.2
		Cys-119	Van der Waals interactions	4.3
				3.0
1g	5.76	His-110	Hydrogen bonding	1.9
		Gln-23	Van der Waals interactions	2.7
1h	7.16	Gly-198	Van der Waals interactions	3.0
		His-110	Hydrogen bonding	2.2
		Trp-221	Aromatic-Aromatic	4.2
1i	6.92	Glu-22	Hydrogen bonding	2.1
		Cys-26	Van der Waals interactions	2.9
		Trp-221	Van der Waals interactions	2.9
1j	7.23	Cys-29	Hydrogen bonding	1.9
		Gln-23	Hydrogen bonding	2.2
		His-199	Van der Waals interactions	2.9
1k	12.17	Cys-119	Sulphur-Lonepair interactions	4.0
		Cys-119	Sulphur-Lonepair interactions	4.3
		His-111	Hydrogen bonding	2.4
				1.9
1l	8.99	Cys-26	Hydrogen bonding	2.2
		Cys-26	Hydrogen bonding	2.6
		Trp-221	Van der Waals interactions	2.1
				2.9
1m	8.83	Glu-122	Hydrogen bonding	2.0

		His-110	Hydrogen bonding	2.2
1n	8.93	Glu-122	Hydrogen bonding	2.0
		His-110	Hydrogen bonding	2.2
		Gln-23	Van der Waals interactions	2.8
1o	7.16	His110	Hydrogen bonding	2.0
		Trp221	Hydrogen bonding	1.9
		Glu-122	Hydrogen bonding	2.4
		Gly-121	Van der Waals	3.0
1p	8.48	Glu- 109	Sulpur -Lonepair interactions	3.8
		His-110	Hydrogen bonding	2.1
		Gly-24	Van der Waals	2.6
1q	11.83	His110	Hydrogen bonding	1.9
		Gly-198	Van der Waals	2.9
1r	11.77	His-110	Hydrogen bonding	1.9
		Gln-23	Hydrogen bonding	2.0
		Trp-221	Hydrogen bonding	2.0
		His-199	Van der Waals	2.8
NS-134	13.41	His110	Hydrogen bonding	1.6
		Gly121	Hydrogen bonding	1.8
		Cys29	Hydrogen bonding	2.3
N-1845	14.52	Gly74	Hydrogen bonding	2.1
				2.0

All the molecular interactions of the synthesized compounds were compared with that of built in ligand, NS-134 and the standard N-1845

Table 4. Molecular docking of the synthesized functionalized azaglycinamides on MAGL.

S.no	LF VS Score	Interacting amino acids	Type of interactions	Bond distance
1a	8.37	Tyr-194	Aromatic-aromatic	4.7
		Arg-57	Hydrogen bonding	2.1
		Glu-53	Hydrogen bonding	2.4
1b	9.80	His-269	Aromatic-aromatic	4.7
		Arg-57	Hydrogen bonding	2.6
		Glu-53	Hydrogen bonding	2.4
1c	8.26	His-269	Aromatic-aromatic	4.8
		Arg-57	Hydrogen bonding	2.4
		Glu-53	Hydrogen bonding	2.2
1d	-13.39	Tyr-194	Aromatic-aromatic	4.7
		Arg-57	Hydrogen bonding	2.0
		Glu-53	Hydrogen bonding	2.2
		Ala-51	Van der Waals	2.9
1e	13.08	Tyr-194	Aromatic-aromatic	4.5
		Arg-57	Hydrogen bonding	1.9
		Glu-53	Hydrogen bonding	2.2
1f	7.67	Tyr-194	Van der Waals	4.4
		Glu-53	Van der Waals	2.9
1g	5.67	Arg-57	Hydrogen bonding	1.9
		Arg-57	Hydrogen bonding	2.2
1h	7.44	His-121	Van der Waals	2.8
		Tyr-194	Aromatic-Aromatic Hydrogen	4.7
		Glu-190	bonding	3.0
1i	6.84	Glu-190	Van der Waals	2.8
		Arg-57	Hydrogen bonding	2.4
		Val-270	Van der Waals	2.9
1j	13.50	Arg-57	Hydrogen bonding	4.0
		Glu-53	Hydrogen bonding	4.3
		His-121	Van der Waals	2.4
1k	13.73	Arg-57	Hydrogen bonding	2.1
		His-121	Van der Waals	3.0
1l	7.65	Glu-53	Van der Waals	3.0
1m	8.69	Glu-190	Van der Waals	2.0
		Glu-190	Sulphur-ion pair	2.8
		Arg-57	Hydrogen bonding	1.8
		Arg-57	Hydrogen bonding	2.1
1n	8.65	Glu-190	Van der Waals	2.0
		Glu-190	Sulphur-ion pair	2.2
		Arg-57	Hydrogen bonding	2.8
		His-121,His-269	Aromatic-aromatic	3.6, 5.1
1o	9.22	Leu-184	Van der Waals	2.9
		Glu-53	Van der Waals	2.9
		Ala-51	Van der Waals	2.4
		Ser-122	Van der Waals	2.7
1p	14.82	Arg-57	Hydrogen bonding	1.8

		Glu-53	Hydrogen bonding	2.3
		Lys-273	Van der Waals	3.0
1q	13.86	Ser-181	Sulphur-ion pair	4.2
		Arg-57	Hydrogen bonding	2.4
		Glu-53	Hydrogen bonding	2.0
		Glu-53	Van der Waals	2.9
1r	8.39	Val-270	Van der Waals	2.9
		Leu-184	Van der Waals	3.0
		Glu-53	Van der Waals	2.8
		Ile-179		
		Glu-53	Aromatic-aromatic	4.8
			Van der Waals	2.8
ZYH	12.18	Tyr-194	Aromatic-aromatic	2.9
		Ala-51	Hydrogen bonding	2.4
		Met-123	Hydrogen bonding	2.3
		Ser-122	Van der Waals	2.8
JZL-195	13.09	Arg-57	Hydrogen bonding	1.9
		Tyr-194	Aromatic-aromatic	4.7
		Leu-205	Van der Waals	2.9
		Ala-51	Hydrogen bonding	2.1

All the molecular interactions of the synthesized compounds were compared with that of built in ligand, ZYH and the standard JZL-195.

Table 5. Antinociceptive studies of synthesized functionalized azaglycinamides.

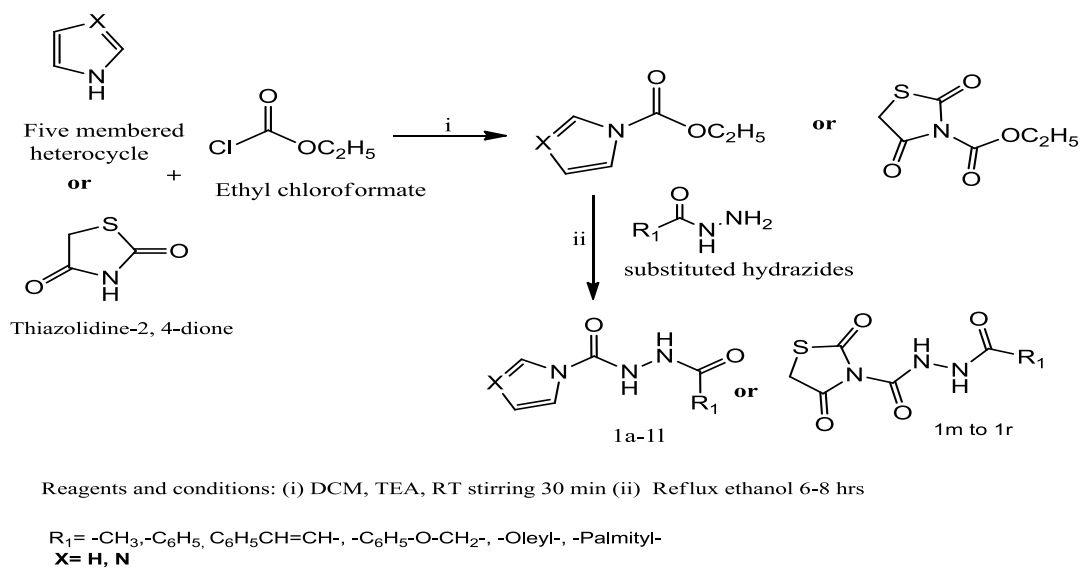
Compound	Eddy's hot plate method ^a (Latency in sec)	Tail immersion method ^a (Latency in sec)	AITC induced nociception ^b	
			No of Lickings / 5 min	No of Flinchings/ 5 min
Control	3.16±0.30	3.16±0.30	23.17±0.44	22.67±0.41
Tramadol/Diclofenac	10.00±0.44*	10.67±0.33*	16.83±0.40*	14.83±0.49*
1e	7.00±0.36*	7.16±0.30*	19.00±0.36*	16.17±0.34*
1k	5.50±0.42*	8.50±0.22*	17.83±0.44*	16.17±0.44*
1q	8.33±0.46*	8.83±0.47*	17.17±0.40*	16.83±0.47*

a Reaction time for jumping/tail with drawl after 1 hr and each value represented as mean± SEM (n=6)

b At 55mg/kg (p.o), no of lickings and flinchings per 5 min were counted after injection of AITC and each value represented as mean± SEM (n=6)

* P<0.05 considered as statistically significant, when compared to control using one way ANOVA in graph pad prism version 7.0

Figures and Schemes:



Scheme 1. Synthetic scheme for the synthesis of functionalized azaglycinamides (1a to 1r).

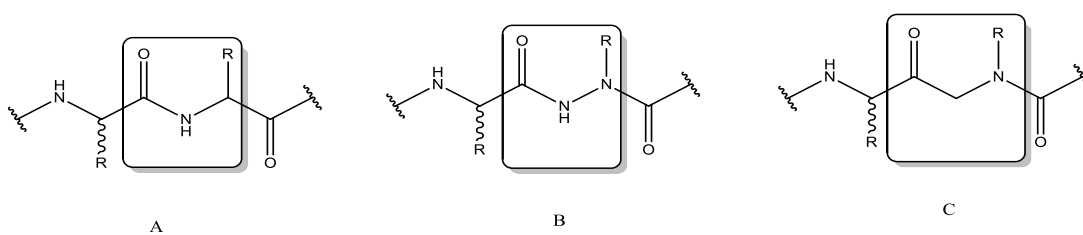


Figure 1. Some important backbone modifications A) Peptide B) Azapeptide C) Peptoid.

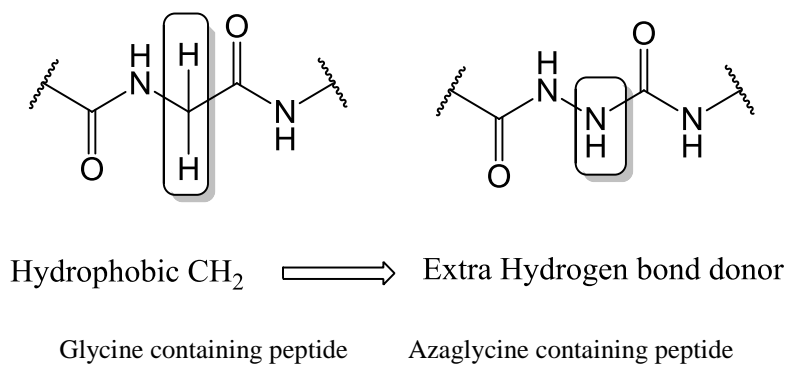


Figure 2. Aza scaffold showing extra hydrogen bond donor property.

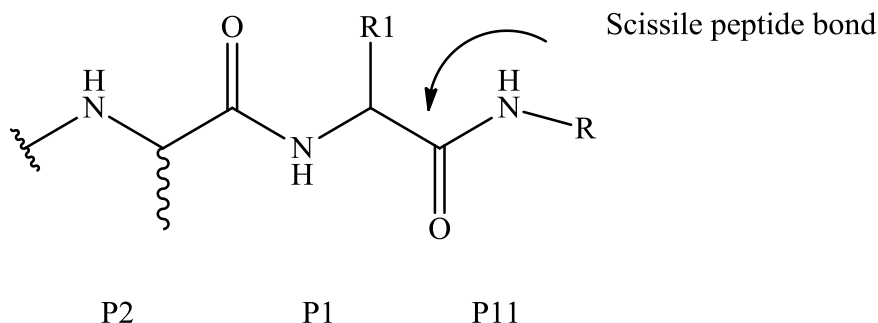


Figure 3. Scissile peptide bond.

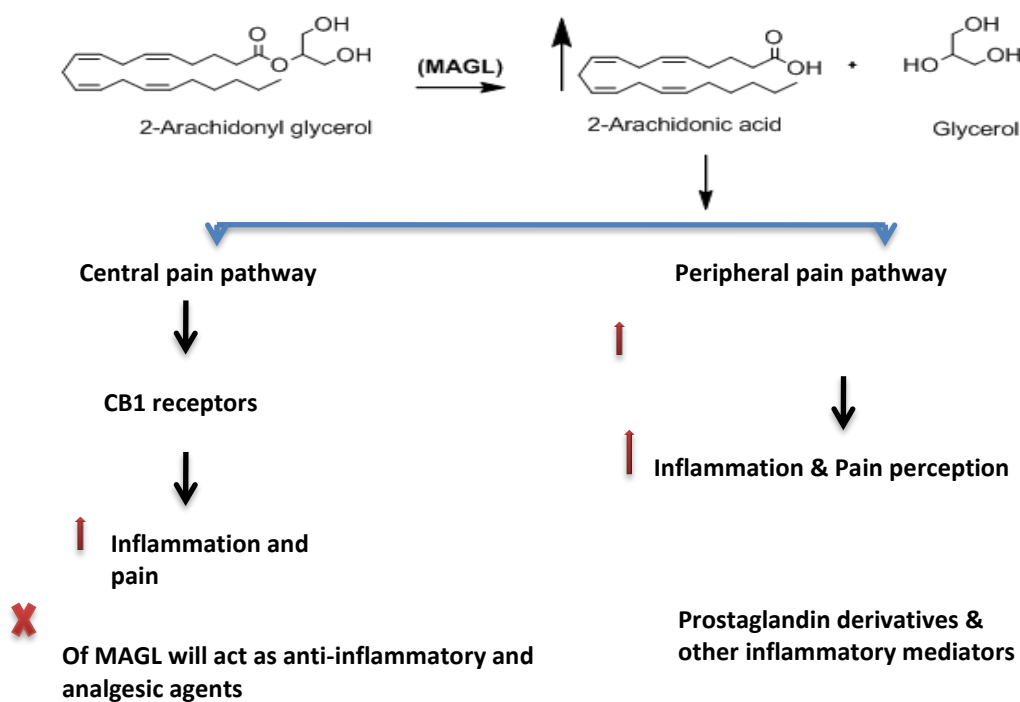


Figure 4. Role of MAGL in inflammatory and pain pathways.

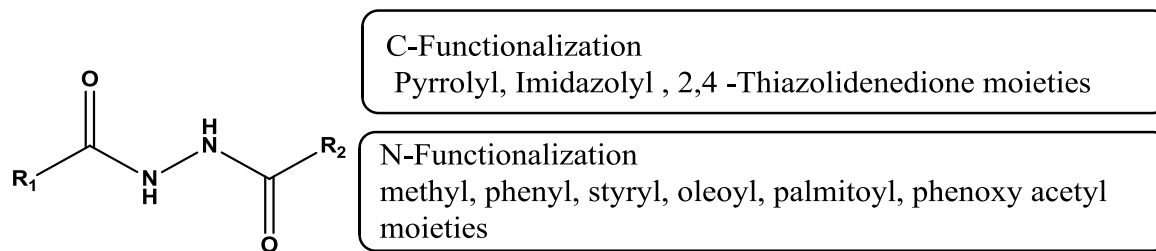


Figure 5. A general depiction of the various modifications on azaglycinyl moiety.

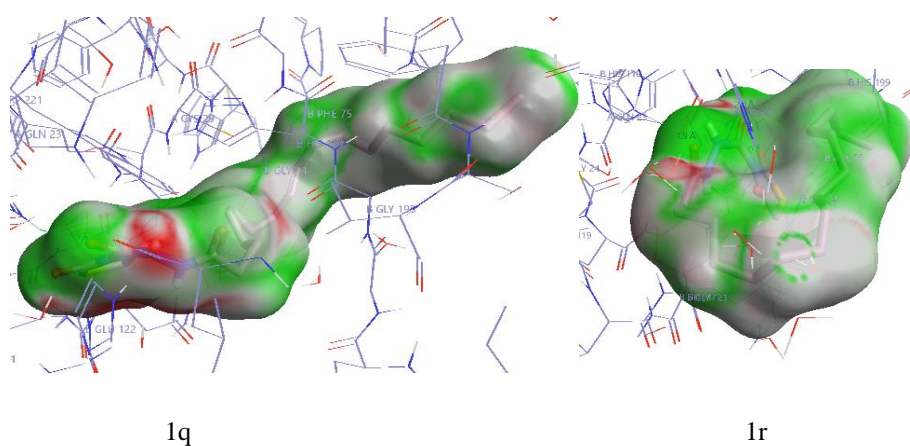


Figure 6. Electrostatic complementarities of 1q and 1r in the active site of Cathepsin B.

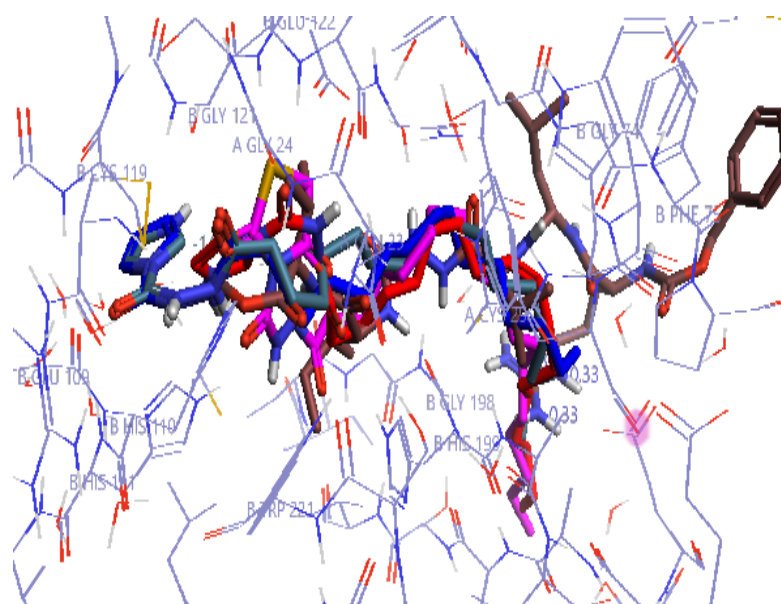


Figure 7. Overlay of active compounds, NS-134, N-1845 in the active site of Cathepsin B. (1q magenta colored; 1l red colored; 1f blue colored; 1k grey color NS-134 green colored N-1845 brown colored).

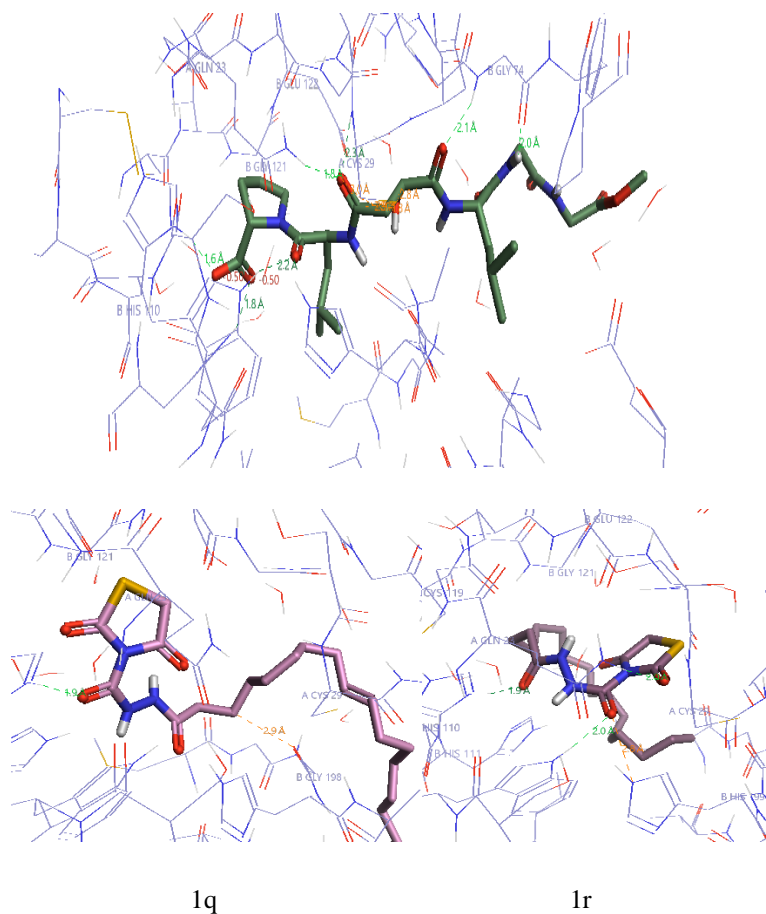


Figure 8. Binding pose of NS-134, 1q and 1r in the active site of Cathepsin B.

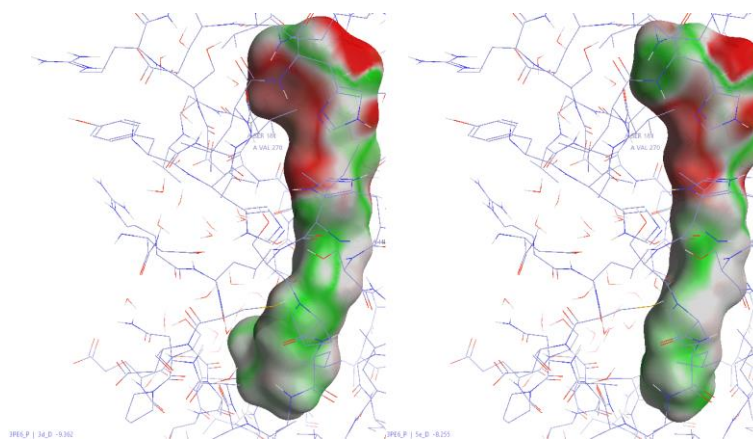


Figure 9. Electrostatic complementarity of 1q and 1e.

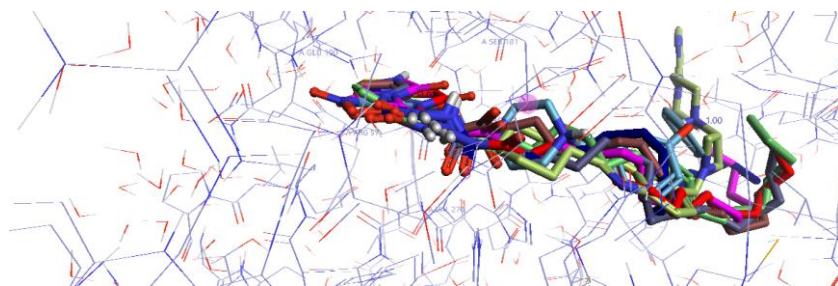


Figure 10. Overlay of compounds in the active site of MAGL.

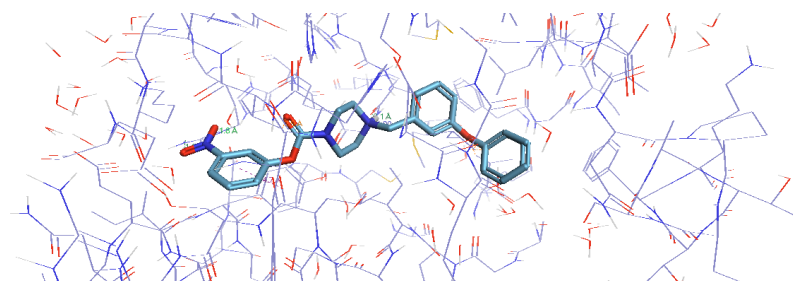
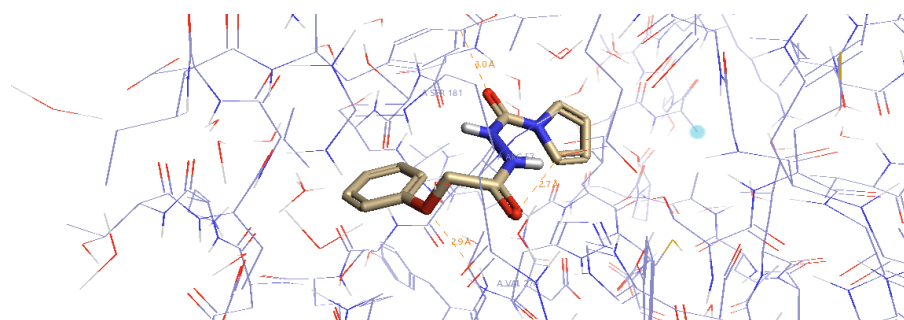
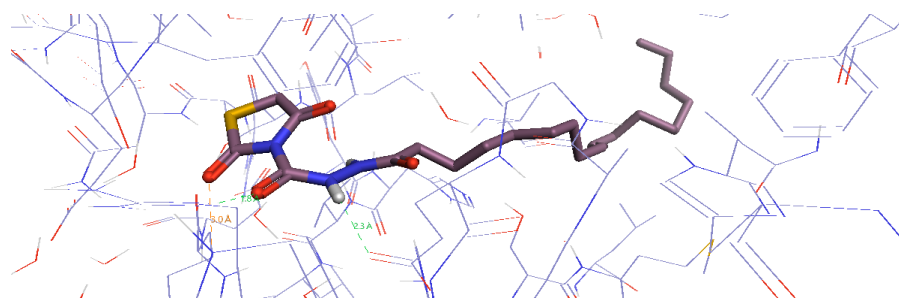


Figure 11. Binding pose of 1e, 1q and JZL195 in active site of MAGL.

ONLINE SUBMISSION

www.ijps.ir